

SYNTHESIS AND CHARACTERIZATION OF CATALYTIC Ni-Cu-Pt/Al₂O₃ MONOLITH FOR HYDROGEN GENERATION VIA AUTOTHERMAL ETHANOL REFORMING

Jéssica Florinda Zeitoune^{1*}, Camilla Daniela Moura Nickel³, Diego Alexandre Duarte², Rafael de Camargo Catapan¹.

¹Laboratory of Applied Catalysis, Joinville Center of Technology, Federal University of Santa Catarina, Joinville, SC, Brazil

²Laboratory of Surface Treatments, Joinville Center of Technology, Federal University of Santa Catarina, Joinville, SC, Brazil

³Federal University of Technology – Paraná

*jessica.zeitoune@posgrad.ufsc.br

ABSTRACT - Growth in electric vehicles (EVs) offers carbon emissions reduction. Ethanol reforming for H₂ production together with fuel cell technologies can extend EVs range. While Pt-based catalysts are effective for ethanol reforming, they are very expensive. On the other hand, Ni and Cu are non-noble catalysts for steam reforming and water gas shift reactions, respectively. In this study, we synthesized and characterized the Ni-Cu-Pt/Al₂O₃ monolith catalyst. Overall, TPR results showed homogeneous catalysts and the availability of Ni, Cu, and Pt for catalysis. SEM revealed efficient active phase impregnation with good dispersion. XRD confirmed alumina and cubic NiO presence, with limited evidence of Cu and Pt contributions. Optimizing these catalysts may enhance hydrogen production and encourage wider H₂ fuel cell use.

Keywords: Ethanol, reforming, hydrogen, catalyst, Ni-Cu-Pt/Al₂O₃

RESUMO - O crescimento dos veículos elétricos (VEs) oferece redução nas emissões de carbono. A reforma do etanol para produção de H₂, junto com tecnologias de células a combustível, pode aumentar a autonomia dos VEs. Embora os catalisadores à base de Pt sejam eficazes na reforma do etano, eles são muito caros. Por outro lado, Ni e Cu são catalisadores não nobres para reações de reforma a vapor e mudança do vapor de água, respectivamente. Neste estudo, sintetizamos e caracterizamos o catalisador monolítico Ni-Cu-Pt/Al₂O₃. No geral, os resultados de TPR mostraram catalisadores homogêneos e a disponibilidade de Ni, Cu e Pt para a catálise. O MEV revelou uma impregnação eficiente da fase ativa com boa dispersão. DRX confirmou a presença de alumina e NiO cúbico, com evidências limitadas das contribuições de Cu e Pt. A otimização desses catalisadores pode aprimorar a produção de hidrogênio e incentivar o uso mais amplo de células a combustível de H₂.

Palavras-chave: Etanol, reforma, hidrogênio, catalisador, Ni-Cu-Pt/Al₂O₃

Introduction

Electric vehicles (EVs) offer a solution for reducing carbon emissions. To enhance their potential, one solution lies in the use of solid oxide fuel cells (SOFCs) powered by H₂, derived from ethanol reforming. Catalysts are crucial for high conversion and selectivity in these reactions (1). Noble metals are effective but expensive, making them less feasible for massive use compared to non-noble metals (2-3). To address this, we have synthesized catalytic Ni-based monoliths, incorporating small quantities of Cu and Pt. Copper promotes coke oxidation, extending catalyst lifespan, while platinum aids in the hydrogenation of carbonyl species and facilitates the breaking of C-C bonds, which also helps reduce coke formation (4-6). Optimizing these catalysts may enhance H₂ production and promote wider H₂ fuel cell usage.

Experimental

Monolith Preparation. Al₂O₃ foams (from GoodFellow), with 26 pores/cm, 12.7 mm thickness, and 80 mm diameter, were used as monoliths. First foams were dried at 110 °C for 1 h. In the coating step, the foam was immersed for 1 min in a paste composed of 40% alumina, 1% sodium silicate, 1% nitric acid, and 58% distilled water, the excess

was removed by dripping for 1 min and the monolith was dried at 110 °C for 1h30min and calcined at 600 °C for 2 h. Ni, Cu, and Pt were sequentially impregnated using an aqueous solutions of Ni(NO₃)₂·6H₂O, Cu(NO₃)₂·3H₂O and H₂PtCl₆·6H₂O with a concentration of 2 M, 0.01 M and 0.016 M, respectively, for 16 h then dried at 150 °C for 12 h with a ramp of 3 °C/min and calcined for 2 h at 600 °C at a rate of 6 °C/min. Nitrate was used as a competing ion added to platinum solution. The concentration of HNO₃ was calculated to achieve [NO₃⁻]:[H₂PtCl₆] ratios of 20:1.

Monolith Characterization. Temperature Programmed Reduction (TPR) was carried out using the QuantaChrome ChemBET Pulsar. The analyses were carried out with a flow of 5% H₂ in N₂, a heating rate of 10 °C/min, and 100 mg of sample material to determine the catalyst's working temperature window and qualitatively compare active metallic phase concentrations on the external (Ext) and internal (Int) parts of the monolith.

Scanning Electron Microscopy (SEM) analysis was conducted for coating homogeneity, impregnation homogeneity, and morphology, using JEOL JSM-6390LV and particle sizes measured via ImageJ.

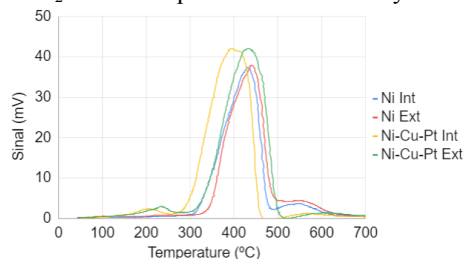
X-Ray Diffraction (XRD) was used to identify crystalline phases and estimate particle sizes using

XRD-6000-SHIMADZU and Cu-K α tubes, a wavelength (λ) of 1.5420 Å, with 2 θ ranging between 10° and 80°, and with a scanning speed of 3 °/min. Analyses were done through Profex 5.2.1. and Origin pro 2016.

Results and Discussion

TPR results shown in Figure 1 the homogeneity of Ni and Ni-Cu-Pt samples, indicated by similar peak heights in the Int and Ext regions of the monoliths. Reduction of NiO was detected in the 300-500 °C range. Ni-Cu-Pt samples showed higher peaks and areas than the Ni sample in the 300-500 °C range indicating the reduction of Cu. Additionally, in the Ni-Cu-Pt samples, is observed a peak around 200-250 °C attributed to the reduction profile of Pt.

Figure 1. H₂ reduction profiles for the catalyst samples.



SEM analysis confirmed effective coating and impregnation. Coverage was mostly homogeneous over the samples. In Figure 4b), particles of around 0.125 μ m were measured. The SEM, however, cannot definitively identify whether these particles are Pt or another metal. Figure 2a), 3a) and 4a) showed there was no visible pore clogging in the samples.

Figure 2. SEM images with alumina coating a) 100x magnification b) 5,000x magnification.

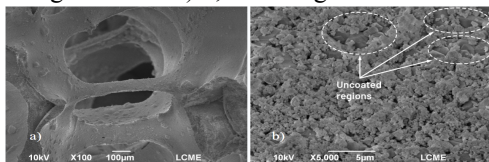


Figure 3. SEM images with Ni impregnation a) 100x magnification b) 10,000x magnification.

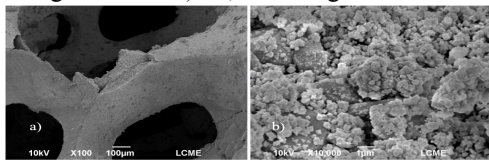
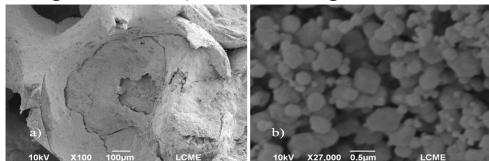


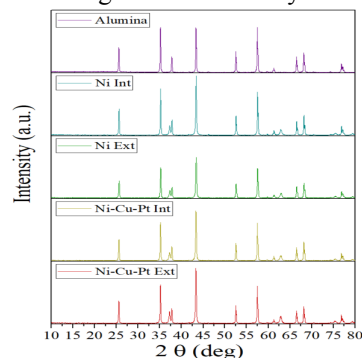
Figure 4. SEM images with Ni-Cu-Pt impregnation a) 100x magnification b) 27,000x magnification.



XRD in Figure 5 showed the most intense alumina peak at a 2 θ of 57.5 with a particle diameter (dp) of 0.05 μ m. Cubic NiO was found in the samples containing Ni, at 2 θ

values of 37.1, 43.1, 62.6, 75.1, and 79.1, with the most intense peak at 2 θ of 43.1 with dp of 0.036 μ m. Low peak intensity for Cu and Pt in Ni-Cu-Pt samples was likely due to their low concentrations. Cu peaks were absent in Ni-Cu-Pt Int samples, while in Ext samples, Cu had a max. Relative Intensity (R.I.) of 1.16% at 2 θ of 43.1. Pt peaks in the Int and Ext samples showed a max. R.I. of 0.32% at 2 θ of 28.0 and 0.84% at 2 θ of 34.9, respectively.

Figure 5. Diffractogram for the catalyst samples.



Conclusions

H₂ reduction profiles settled that the three metals were reduced. SEM revealed consistent coatings and impregnation layers, with minor uncoated areas. XRD analysis confirmed alumina and cubic NiO structures but indicated limited Cu and Pt contributions. Scale disparity between SEM and XRD affects dp measurements. SEM gave insight into potential agglomeration of crystallites, while XRD provided an atomic-scale perspective, potentially revealing smaller crystallite sizes than SEM.

Acknowledgments

The authors are thankful for the Multi-User Facility infrastructure from UDESC. D. A. Duarte thanks the financial support from CNPq (grant no. 307408/2021-3). This work was funded by FUNDEP Rota2030, BMW Brazil Group, AVL South America and Agora Tech Park under the project 27192*17.

References

1. L. Guerrero; S. Castilla; M. Cobo, *Quím. Nova* **2014**, 37, 850-856.
2. S. Ogo; Y. Sekine, *Fuel Process. Technol.* **2020**, 199, 106-238.
3. R. Baruah; M. Dixit; P. Basarkar; D. Parikh; A. Bhargav, *Renew. Sustain. Energy Rev.* **2015**, 51, 1345-1353.
4. Y. C. Sharma; A. Kumar; R. Prasad; S. N. Upadhyay, *Renew. Sustain. Energy Rev.* **2017**, 74, 89-103.
5. A. J. Vizcaíno; A. Carrero; J. A. Calles, *Int. J. Hydrog. Energy.* **2007**, 32, 1450-1461.
6. R. B. Sierra; J. R. Martínez; J. C. S. Ruiz; F. R. Reinoso; A. S. Escribano, *J. Colloid Interface Sci.* **2012**, 383(1), 148-154.